



Science Arts & Métiers (SAM)

is an open access repository that collects the work of Arts et Métiers Institute of Technology researchers and makes it freely available over the web where possible.

This is an author-deposited version published in: <https://sam.ensam.eu>
Handle ID: <http://hdl.handle.net/10985/10042>

To cite this version :

Cécile COURGNEAU, Sandra DOMENEK, Régis LEBOSSÉ, Alain GUINAULT, Luc AVÉROUS, Violette DUCRUET - Effect of crystallization on barrier properties of formulated polylactide - Polymer International - Vol. 61, p.180–189 - 2012

Any correspondence concerning this service should be sent to the repository

Administrator : scienceouverte@ensam.eu



Effect of crystallization on barrier properties of formulated polylactide

Cécile Courgneau,^{a,b} Sandra Domenek,^b Régis Lebossé,^c Alain Guinault,^d Luc Avérous^e and Violette Ducruet^{a*}

Abstract

Poly(lactide) (PLA), a biodegradable polymer obtained from biomass, was formulated with a nucleating agent, talc, and a plasticizer, acetyl tributyl citrate, and cold crystallized in α and α' form. The barrier properties of crystallized PLA were investigated as a function of the formulation and the crystalline form, thanks to three molecules with increasing polymer interactions, i.e. helium, oxygen and ethyl acetate (EA). Contrary to expectation, the oxygen diffusion coefficient in neat and formulated PLA did not decrease with crystallization. Even an increase of the diffusion coefficient was noticed for the most interacting probe, EA, in formulated PLA. Conditioning of neat and formulated PLA in an atmosphere containing EA vapour caused a modification of the material structure by plasticization and induced crystallization even at small EA activities. The plasticizing effect caused the glass transition temperature T_g to shift to below ambient temperature. In the case of neat PLA induced crystallization in solely the α form was obtained, and in the case of formulated PLA a blend of α and α' forms was observed.

Keywords: polylactide; poly(lactic acid); crystallization; formulation; permeability; solvent-induced crystallization (SINC)

INTRODUCTION

Due to their environmental merits, biomass-based polymers have been widely studied, particularly polylactide (PLA). The subject of an increasing number of publications, PLA presents great interest for industrial and commodity application.^{1–3} Worldwide production capacity is dramatically increasing from 74 kt p.a. in 2003 to 229 kt p.a. in 2009 and should amount to 833 kt p.a. in 2020.⁴

Ease of processing, good mechanical properties, high glass transition temperature and high transparency make PLA a promising material for packaging or containers. However, its high brittleness and poor barrier properties restrict its application domain. The last-mentioned properties are required, for example, for packaging to preserve organoleptic food quality during shelf life by preventing alteration of food due to excessive oxygen or water vapour transfers or loss of aromatic compounds.^{5,6}

The gas barrier properties of neat PLA have already been studied, but mainly for amorphous films.^{7–9} The oxygen barrier properties of amorphous PLA are similar to those of high density poly(ethylene) (HDPE) and intermediate between poly(ethylene terephthalate) (PET) and polystyrene (PS).^{10–13} Unlike gases, the organic molecule barrier properties of PLA have been less extensively studied.^{11,14–16} Auras *et al.*¹⁴ showed that the solubility coefficient of limonene in PLA is lower than that in PET, PS, polypropylene (PP), HDPE and low density poly(ethylene) (LDPE).¹⁶ Ethyl acetate (EA), a solvent largely used in inks and adhesives, showed in contrast a comparatively higher solubility coefficient in PLA. To give an example, the solubility coefficient of EA can be twofold higher in PLA than in PET, PP and LDPE.

One way to improve the barrier properties of semicrystalline polymers is to increase their crystallinity. Crystalline zones are

presumed to be excluded volumes through which molecules cannot diffuse and in which they cannot sorb,¹⁷ in contrast to amorphous zones where diffusion is possible. However, according to the study of Kanehashi *et al.*¹⁸ on 300 crystalline or liquid crystalline polymers, the permeability and diffusion coefficients of gas are not significantly affected by crystallinity at low crystallinity degree. The influence of crystallinity on the barrier properties has been rarely studied for PLA and has led to contradictory results due to the lack of knowledge about the crystalline structure of the materials studied, in particular in the case of P(D,L)LA.

The crystalline morphology of PLA depends on its stereochemistry,¹⁹ crystallization kinetics^{20,21} and temperature (T_c), and its thermal history (cold or melt crystallization).^{22–24}

Furthermore, PLA is known for its low crystallization rate.^{28,31} Nevertheless, similarly to other semicrystalline polymers, decreas-

* Correspondence to: Violette Ducruet, INRA UMR 1145 Ingénierie Procédés Aliments, 1 avenue des Olympiades, F 91300 Massy, France.
E-mail: violette.ducruet@agroparistech.fr

a INRA UMR 1145 Ingénierie Procédés Aliments, 1 avenue des Olympiades, F 91300 Massy, France

b AgroParisTech UMR 1145 Ingénierie Procédés Aliments, 1 avenue des Olympiades, F 91300 Massy, France

c LNE, Laboratoire national de métrologie et d'Essais, 29 avenue Roger Hennequin, 78197 Trappes CEDEX, France

d CNAM, Laboratoire P2AM, 292 rue Saint-Martin, case courrier 322, 75141 Paris CEDEX 03, France

e ECPM-LIPHT, EAC (CNRS) 4379, Université de Strasbourg, 25 rue Becquerel, 67087 Strasbourg CEDEX 2, France

ing the nucleation activation energy and increasing the mobility of the chain segments are key elements to increasing the PLA crystallization rate.^{25–27} An efficient way to decrease the nucleation activation is to add a nucleating agent whereas the mobility of the chain segment can rise due to the addition of plasticizer.

Several nucleating agents have been tested on PLA. An example is the stereocomplex of P(L)LA and P(D)LA,^{28,29} which induces a decrease of the crystallization half-time of P(L)LA at an incorporation content less than 10 wt%. Some research has shown that organic compounds can be successful in playing the role of a nucleating agent. *N,N*-ethylene-bis-12-hydroxystereamide leads to an increase of the nucleation density (multiplied by 10) and crystallization rate (from 5 to 20 times).^{30,31} Kawamoto *et al.* have shown that other organic compounds based on hydrazide groups can increase the crystallization temperature upon cooling.³² Other nucleating agents, such as sodium salts, calcium lactate, CaCO₃, TiO₂ and BaSO₄, have demonstrated a lower efficiency.^{33,34} Data show that these substances are less efficient than talc, which is widely used as a nucleating agent since the crystallization rate is 65-fold higher than that of PLA alone.^{31,34,35}

Various types of plasticizers have been used to modify the PLA properties, such as oligomeric lactic acid,³⁶ triacetin,³⁷ diethyl bishydroxymethyl malonate,³⁸ poly(1,2-butanediol), dibutyl sebacate acetyl glycerol monolaurate,³⁹ triphenyl phosphate,²⁵ polyadipates,^{40,41} poly(propylene glycol),^{42,43} poly(ethylene glycol)^{36,43–46} and acetyl tributyl citrate.^{37,44,47,48} The majority of these plasticizers are approved for food contact.^{49,50} According to the literature, acetyl tributyl citrate (ATBC) seems to be the most efficient plasticizer because, in addition to being approved by the US Food and Drug Administration, it efficiently decreases the glass transition temperature and improves significantly the mechanical properties of PLA.^{44,47,48,51}

Consequently, the formulation of PLA with both talc and ATBC appears as a good way to increase the crystallization rate of PLA and should induce an improvement of the barrier properties. The purpose of this paper is to assess the relationships between the crystallization and the gas (helium and oxygen) and EA barrier properties of neat and formulated P(D,L)LA. The mechanical properties were also tested on neat and formulated PLA, before and after annealing. The crystalline structure of the neat and formulated recrystallized PLA was determined by DSC and with wide angle X-ray diffraction (WAXD).

EXPERIMENTAL

Materials

The PLA pellets were provided by NatureWorks (Minnetonka, USA). The content of L-lactide was about 92 wt%. The weight average molecular weight was 9.0×10^4 g mol⁻¹ with a dispersity (*D*) of 2.75.

ATBC, used as a plasticizer, was purchased from Sigma Aldrich (Saint Quentin Fallavier, France). Talc, used as a nucleating agent, was provided by RioTinto (Luzenac, France). EA and hexadecane were supplied by Sigma Aldrich (Saint Quentin Fallavier, France).

Sample preparation

PLA pellets, plasticizer and nucleating agent were dried at 80 °C overnight in a vacuum oven. After that, the formulated PLA samples were prepared by direct melt mixing of the additives with PLA in an internal mixer (Haake Rheocord 9000) at 160 °C and 60 rpm for 15 min. Concentrations of ATBC and talc were 17 wt% and 1 wt% in the blend, respectively.

To decrease the water content, the materials were dried for 4 h minimum at 80 °C before processing. PLA samples were transformed by thermo-compression (Telemechanique, 15 t) at 185 °C and 150 bars (15 GPa) to obtain a film of approximately 300 μm thickness. After compression, the films were quenched to ambient temperature. Non-annealed films were stored at ambient temperature in a desiccator with P₂O₅.

The films were annealed in an air-circulating oven (Angeltoni Climatic System Massa Martana Type TY80) at the recrystallization temperature (90 or 120 °C for neat PLA and 85 or 100 °C for the formulated one) for different durations (90 min for neat PLA and 10, 30 or 60 min for the formulated one).

Conditioning of PLA film in EA atmosphere

The annealed PLA film samples were equilibrated in an EA atmosphere at 0.2 and 0.5 activity for 2 weeks in a hermetic vessel at 25 °C using the method published by Colomines *et al.*¹¹ The 0.2 and 0.5 activities were generated by 0.8 and 2.2 mol L⁻¹ EA solutions in hexadecane, respectively, and controlled by gas chromatography. The activity is the ratio p/p_0 with p the partial pressure and p_0 the vapour pressure of EA at saturation.

Analysis methods

DSC

The thermal analyses were performed with an MDSC Q100 (TA Instruments) under a nitrogen atmosphere. The samples (about 10 mg) were put into hermetic aluminium pans (TZero, TA Instruments). The standard mode was used to measure isotherms from the cold state and to study the crystallization.

To investigate the kinetics of isothermal crystallization, neat and formulated PLA were heated at 190 °C for 10 min to erase the thermal history of the sample and then cooled to 20 °C and reheated to the crystallization temperature at 50 °C min⁻¹. Hence the isothermal crystallization begins from 15 min.

The half-time of crystallization, $t_{1/2}$, is defined as the time at which half of the final crystallinity is developed. After 3 h of crystallization, the sample is cooled to room temperature. Finally the sample is heated at 10 °C min⁻¹ to 190 °C to determine the melt temperature. The equilibrium melting temperatures of neat and formulated PLA are the intersection of the straight line $T_m = f(T_{cc})$ with the line $T_m = T_{cc}$. A baseline was carried out with a sapphire at each temperature with the same thermal programme as for the PLA samples.

For analysing the degree of crystallinity of the samples (χ_c), heating scans were performed at a heating rate of 10 °C min⁻¹ from -30 to 190 °C. The χ_c of neat PLA was calculated from Eqn (1), where ΔH_m is the enthalpy of melting, ΔH_{cc} is the enthalpy of cold crystallization and ΔH_m^0 is the enthalpy of fusion per gram of a perfect crystal of infinite size, i.e. 93 J g⁻¹.⁵²

$$\chi_c = \frac{\Delta H_m - \Delta H_{cc}}{\Delta H_m^0} \quad (1)$$

The equivalent degree of crystallinity (χ_{ce}) of formulated PLA was calculated using Eqn (2) where x_{PLA} is the weight fraction of PLA in the formulated PLA:

$$\chi_{ce} = x_{PLA} \times \frac{\Delta H_m - \Delta H_{cc}}{\Delta H_m^0} \quad (2)$$

All experiments were carried out in triplicate.

SEC

The average molecular weights were measured by SEC using a Shimadzu apparatus equipped with an RID-10A refractive index detector and an SPD-M10A UV detector. The analyses were carried out at 30 °C and 0.8 mL min⁻¹ in chloroform on a PL Gel 5 µm Guard column and two PL Gel 5 µm Mixed-C columns. The calibration was performed with PS standards from 580 to 1 650 000 g mol⁻¹.

WAXD

The WAXD experiments were conducted at 50 kV, 35 mA, using Cu K α radiation monochromatized with a graphite monochromator (Panalytical, X'Pert Pro MPD). The diffractograms were recorded for 2θ angles between 5° and 35° with a step size and time of 0.007° and 368.8 s, respectively.

The degree of crystallinity of the samples was calculated by the surface method. The ratio of the amorphous halo and the total surface of the spectrum was carried out to retrieve the amorphous phase fraction and then to find the crystallinity degree.

Tensile test

Uniaxial tensile testing was carried out at room temperature and at 5 mm min⁻¹ with an Instron tensile testing machine (Instron Model 4507) equipped with pneumatic jaws on type IBA dumbbell-shaped samples. The thickness of the samples varied from 200 to 300 µm. Each value is an average of five measurements.

Oxygen, helium and water vapour permeability

The direct measurement of the oxygen transmission rate was monitored at 23 °C and 0% relative humidity (RH) with a Systech 8001 apparatus. The helium transmission rate was measured at room temperature and at a relative humidity varying between 40% and 60% RH, by a specific analyser developed by CNAM (Paris, France), based on the ISO norm 15105-2 : 2003. Oxygen and helium permeabilities were then obtained by dividing the oxygen transmission rate and helium transmission rate respectively by the film thickness. Experiments were carried out in duplicate. The diffusion coefficients (D) were estimated by the time lag method according to Eqn (3), where l is the film thickness and θ the time lag. The time lag is determined as the intercept of the time axis and the extrapolated linear steady state part of the curve for a representation of the amount of permeant passing through the film in time t versus time.

$$D = \frac{l^2}{6\theta} \quad (3)$$

In the helium case, the time lag accounted only for a few seconds causing poor repeatability in its determination. Consequently, the helium diffusion coefficient presented in this work is an approximate value to tentatively compare its order of magnitude with the diffusion coefficient of the other probes.

The solubility coefficients (S) were calculated using the general equation

$$P = D \times S \quad (4)$$

where P is the gas permeability.

EA sorption kinetics

The sorption isotherm of EA was measured at 25 °C and 0% RH with a static method, using an electronic microbalance (Intelligent Gravimetric Analyzer 002, Hiden Isochema Ltd, Warrington,

UK) with a sensitivity of 0.2 µg. The film samples (30–60 mg) were suspended from the microbalance by a stainless steel spiral which was contained in a thermoregulated cell, at 25 °C. The microbalance was maintained at 50 °C to ensure stability during the weight measurement by the prevention of solvent condensation. Before the measurement, the samples were purged for 24 h at 10⁻⁵ mbar to remove all volatile compounds sorbed in the film and present in the chamber. Then the EA partial pressure was set using a pressure transducer (Baratron®, MKS Instruments, Wilmington, MA, USA) linked to a tank with a vapour phase saturated in EA. The weight uptake of the sample was recorded automatically against time at 0.2 activity.

The apparent EA solubility S_{app} (kg m⁻³ Pa⁻¹) was calculated according to

$$S_{app} = m_{\infty} \times \frac{d}{p} \quad (5)$$

where m_{∞} is the equilibrium sorption obtained theoretically after infinite time (kg kg⁻¹), d is the film density (kg m⁻³) and p the compound vapour partial pressure (Pa). Each sample was measured in duplicate. The microbalance is calibrated regularly during maintenance periods for pressure, weight and temperature. The used methods were previously published by Colomines *et al.*¹¹

Estimation of EA diffusion coefficient

In the case of formulated PLA, the diffusion coefficient was calculated from

$$\frac{m_t}{m_{\infty}} = \left(\frac{16 \times D}{\pi \times l^2} \right)^{1/2} \sqrt{t} \quad (6)$$

where m_{∞} is the equilibrium sorption obtained theoretically after infinite time (kg kg⁻¹), m_t is the weight at time t (s), l the thickness of the film (m) and D the diffusion coefficient (m² s⁻¹). In the case of neat non-annealed and recrystallized PLA, the equilibrium was not reached. Consequently the diffusion coefficients were estimated using Eqn (6) from equilibrium state experiments carried out at higher temperature.

Statistical analysis

The statistical analysis was done with a one-way analysis of variance (ANOVA). When the differences were significant ($P < 0.05$), Fischer's test was used to check the differences between pairs of groups and was carried out using XLSTAT-Pro 7.0 software (Addinsoft, Paris, France). Statistical analysis was carried out separately for neat PLA and formulated PLA.

RESULTS AND DISCUSSION

Optimization of crystallization conditions

The melting temperatures versus the cold crystallization temperatures for neat and formulated PLA are plotted in Fig. 1. The equilibrium melting temperature determined was 173.5 °C for neat PLA. This temperature decreases with the addition of ATBC and talc to 163.5 °C. The melting point depression is noticeably higher than the one reported by Xiao *et al.* with 15 wt% triphenyl phosphate in PLA.⁵³

According to the literature,^{54–57} PLA may crystallize during thermal treatment in two forms, the α and α' forms. A higher crystallization temperature ($T_c > 130$ °C) induces the formation of the α form whereas a low T_c (80 °C $< T_c < 110$ °C) leads to

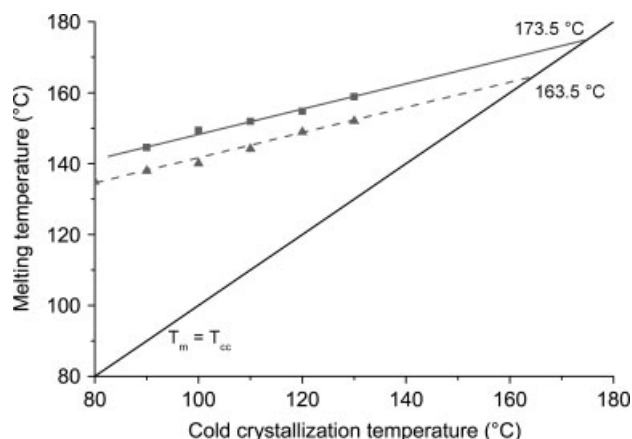


Figure 1. Hoffman –Weeks plots for neat (■) and formulated (▲) PLA.

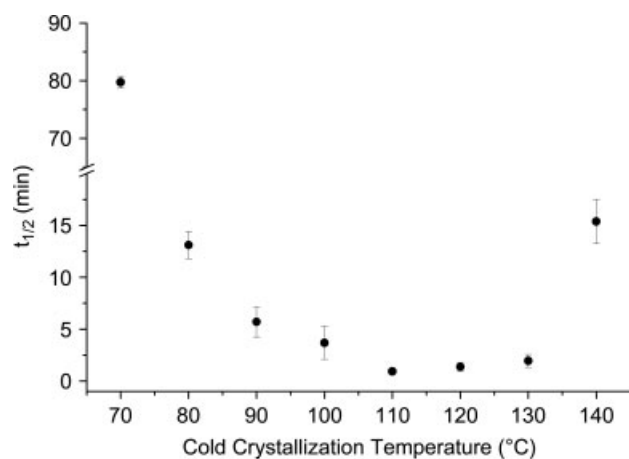


Figure 2. Half-time of crystallization of neat PLA (nPLA) as a function of isothermal cold crystallization temperature.

the formation of the α' form (disordered α form). In the range 110–130 °C, the α and α' forms coexist.^{54–56}

To evaluate the influence of the polymorphism with a constant crystallinity degree on the mechanical and barrier properties, two cold crystallization temperatures were chosen for neat PLA: 90 °C to obtain the α form and 120 °C to ensure the formation of the ordered and disordered α form. The degree of undercooling of neat PLA is evaluated at 54 and 35 °C for 90 and 120 °C, respectively.

As the melting temperature decreases with the formulation, lower cold crystallization temperatures, 85 and 100 °C, were selected to crystallize the formulated samples in the oven. The degree of undercooling of formulated PLA is then evaluated at 52 and 40 °C for 85 and 100 °C, respectively.

The half-time of crystallization ($t_{1/2}$) of neat PLA measured in isothermal conditions after cooling from the melt is plotted in Fig. 2 as a function of the cold crystallization temperature. The optimum $t_{1/2}$, 1.5 min, is measured at 110 °C.

Crystallization isotherms were performed by DSC to determine the crystallization duration to obtain fully crystallized samples. As shown in Fig. 3, the crystallization peak time of neat PLA was observed at 5.9 and 0.5 min, at 90 and 120 °C, respectively. Moreover, as shown in Fig. 2, the half-time of crystallization, at 90 and 120 °C, is below 5 min. Hence, to ensure full crystallization of the sample in the oven, the annealing time was chosen to

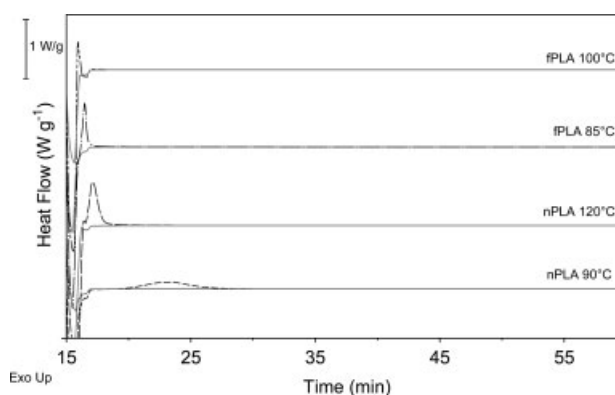


Figure 3. DSC thermograms for neat (nPLA) and formulated PLA (fPLA) (black lines) during isothermal cold crystallization at 90 and 120 °C for neat PLA and 85 and 100 °C for formulated PLA. The baselines, obtained with sapphire at each crystallization temperature, are grey lines. The curves were vertically shifted for legibility.

be more than 20 times the neat PLA $t_{1/2}$, i.e. for 90 min at both temperatures.

As expected, the formulation increases the crystallization rate. The isotherms of the formulated PLA show a sharp peak at 0.1 min at 85 °C (Fig. 3). In the case of crystallization at 100 °C, the crystallization peak was completed after 1.5 min, a time which was completely inside the phase of temperature stabilization of our DSC apparatus. To assess the influence of crystallization duration and crystal perfection, the formulated samples were crystallized for 10 and 30 min at 85 °C and 10, 30 and 60 min at 100 °C, which is much larger than the presumed half-time of crystallization of formulated PLA.

Characterization of the crystal structure and mechanical properties

Results obtained on the crystallinity of the neat and formulated PLA samples recrystallized in the DSC apparatus or annealed in the oven are listed in Table 1. The DSC data show an increase in crystallinity with recrystallization temperature for the neat PLA. Film samples annealed in the oven show smaller crystallinity, most probably due to a less well controlled temperature. In the case of DSC annealing the crystallinity degree reached 52%, whereas in the oven the maximum was recorded at 43%. The crystallization conditions did not lead to a change in the crystallinity degree of the formulated PLA. The crystallinity degree reached around 31% whatever the crystallization temperature and duration, which was lower than that observed in the case of the neat sample. A decrease in crystallinity with plasticization was also observed by Xiao *et al.*⁵⁸ for PLA-based blends with triphenyl phosphate. The formulated samples annealed at 85 °C for 10 min showed discrepancy between the DSC experiment and samples annealed in the oven, which could be attributed to a temperature gradient in the oven.

PLA is highly sensitive to thermal treatments which may induce a decrease in the molecular weight^{59,60} mainly due to hydrolysis. Therefore, the polymer molecular weights were determined and are given in Table 1. The weight average molecular weights of neat and formulated PLA film are 103 000 and 83 000 g mol⁻¹ respectively, indicating a degradation phenomenon during the blending step. No significant decrease in molecular weight is noticed during the annealing in the oven for the different systems.

Table 1. Crystallinity degree of neat and formulated PLA samples after recrystallization in the DSC oven and in the ventilated oven; number and weight average molecular weight (M_n and M_w) of PLA pellets, non-annealed and recrystallized neat and formulated PLA; and mechanical properties of the neat and formulated PLA samples, before and after recrystallization

	Recrystallization conditions	Notation of the samples	Crystallinity degree (%)		M_n (g mol ⁻¹)	M_w (g mol ⁻¹)	Stress (MPa)	Elongation at break (%)	Young's modulus (MPa)
			In the DSC apparatus	In the oven					
PLA pellets									
	Non-annealed	(a)	—	—	90 500	248 900	—	—	—
	90 °C, 90 min	(b)	—	—	55 350	103 100	40.9 ± 3.5 ^a	5 ± 2 ^a	1398 ± 23 ^a
Neat PLA	120 °C, 90 min	(c)	46	36 ± 2	56 850	109 900	46.4 ± 8.3 ^a	5 ± 2 ^a	1216 ± 106 ^b
			52	43 ± 1	66 250	122 050	53.0 ± 1.0 ^b	5 ± 1 ^a	1287 ± 22 ^b
	Non-annealed	(d)	—	—	44 000	82 800	15.8 ± 0.8 ^a	477 ± 20 ^a	38 ± 16 ^a
	85 °C, 10 min	(e)	37	3 ± 3	55 350	106 050	19.4 ± 4.4 ^b	523 ± 103 ^a	84 ± 24 ^b
	85 °C, 30 min	(f)	38	32 ± 1	54 450	93 500	20.0 ± 2.6 ^b	59 ± 24 ^b	347 ± 21 ^d
Formulated PLA	100 °C, 10 min	(g)	38	31 ± 1	43 100	74 850	18.9 ± 0.4 ^b	86 ± 22 ^b	304 ± 13 ^c
	100 °C, 30 min	(h)	n.d.	31 ± 2	41 000	93 950	19.7 ± 1.8 ^b	59 ± 30 ^b	379 ± 53 ^e
	100 °C, 1 h	(i)	39	30 ± 1	48 500	107 550	18.9 ± 1.1 ^b	66 ± 32 ^b	349 ± 32 ^{d,e}

n.d., not determined.

^{a,b,c,d,e} Different letters indicate significant differences at $P < 0.05$ (Fischer); Statistical analysis was carried out separately for neat PLA and formulated PLA.

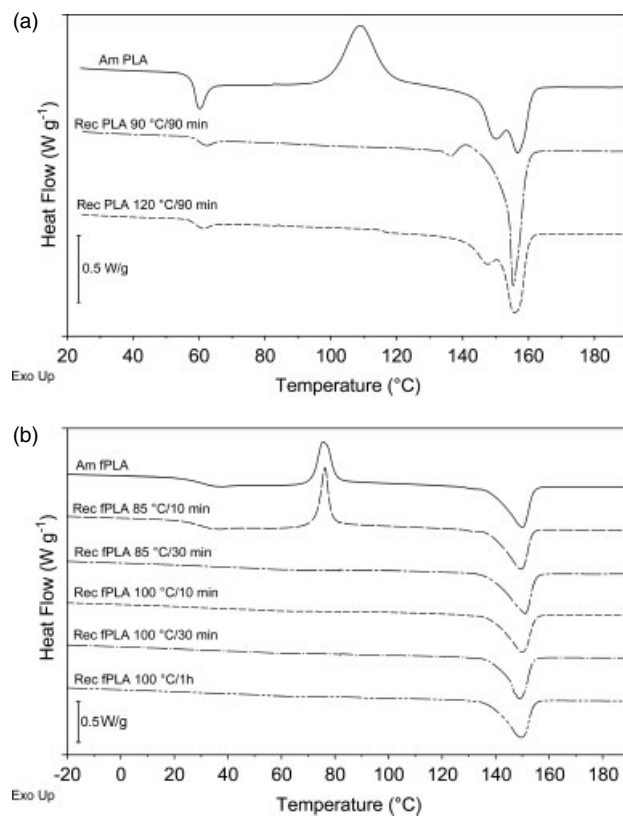


Figure 4. DSC thermograms for neat PLA (a) and formulated PLA (b) heated at 10 °C min⁻¹ after isothermal cold crystallization. The curves are vertically shifted for legibility.

Figure 4 shows the thermograms of neat and formulated PLA after recrystallization in the oven. The melting behaviour depends on the crystallization temperature and consequently on the crystal form. As shown in Fig. 4(a), the non-annealed neat PLA shows cold crystallization during heating. The exotherm is followed by two endotherms spanning from 140 to 160 °C. The sample recrystallized at 90 °C displays a small exotherm prior to the single melting endotherm whereas the sample recrystallized at 120 °C shows a double melting peak. According to Pan and Inoue,⁵⁴ the exotherm prior to the melting peak is due to transformation of the α' form crystal into α form upon heating. The explanation is different for the usual double endotherm. According to Shieh and Liu,⁶¹ the occurrence of the double melting peak may be explained by a melting–recrystallization mechanism. They suggest that the first melting peak is due to the melting of crystals formed during heating or during the recrystallization step at a temperature between 110 and 130 °C while the second peak corresponds to the melting of the more perfect crystals which were formed in the partially molten material.

Figure 4(b) shows the thermograms of the non-annealed and recrystallized formulated PLA. As expected, the formulation of the non-annealed and amorphous PLA induces a decrease in the temperature of the thermal transitions compared with the non-annealed and amorphous neat PLA (Fig. 4). The plasticizer addition leads to an increase in the free volume and a decrease in the polymer chain interactions which yields higher chain mobility at lower temperature. Then, the glass transition temperature of the non-annealed samples drops from 58.1 to 28.6 °C with the formulation (Table 2)

Samples	Recrystallization conditions	Glass transition (°C)			Equivalent crystallinity degree (%) by DSC			Crystallinity degree (%) by WAXS			Crystalline form	
		Before EA contact	After EA contact 0.2 activity	After EA contact 0.5 activity	Before EA contact	After EA contact 0.2 activity	After EA contact 0.5 activity	Before EA contact	After EA contact 0.5 activity	Before EA contact	After EA contact 0.5 activity	
Neat PLA	Non-annealed	58.1 ± 1.2	27.1 ± 0.8	19.5 ± 2.3	3 ± 1	26 ± 1	37 ± 4	0.5	33	–	α	
	90 °C, 90 min	58.7 ± 0.7	n.d.	20.3 ± 1.1	36 ± 2	n.d.	30 ± 1	31	35	α'	α'	
	120 °C, 90 min	58.4 ± 0.7	59.3 ± 0.3	19.6 ± 0.7	43 ± 1	44 ± 1	39 ± 2	40	43	α	α	
Formulated PLA	Non-annealed	28.6 ± 0.6	8.3 ± 0.2	4.4 ± 0.1	2 ± 1	38 ± 4	41 ± 1	2	21	–	α, α'	
	85 °C, 30 min	25.1 ± 3.2	16.4 ± 0.1	9.8 ± 0.1	39 ± 1	41 ± 1	38 ± 1	34	34	α, α'	α, α'	
	100 °C, 1 h	24.6 ± 3.0	16.4 ± 0.2	11.3 ± 0.7	37 ± 1	40 ± 1	35 ± 1	38	41	α, α'	α, α'	
n.d., not determined.												

whereas the cold crystallization temperature decreases from 110 to 80 °C.

The formulated recrystallized PLA samples display no cold crystallization peak, except for 85 °C/10 min. The crystallization peak between 70 and 80 °C is followed by the melting peaks, a small one around 130 °C and the dominant one at 150 °C. This double endotherm is also visible for the sample recrystallized 10 min at 100 °C. Apparently, short recrystallization durations do not allow for crystal perfection and therefore show a melting–recrystallization phenomenon, whereas at longer duration perfect α forms are obtained.

The WAXD patterns of neat and formulated recrystallized samples are depicted in Fig. 5. Distinct diffraction peaks were observed for the neat recrystallized samples according to the annealing temperature. As given in the literature,^{54–56,62} the samples recrystallized at 90 °C exhibit an α' crystal structure characterized by intense peaks at 16.5° and 18.9°, due to the diffraction from (200) and/or (110) planes and from the (203) plane, respectively. Weak reflections are also observed at 12.3°, 14.7° and 22.2° due to diffraction from the (103), (010) and (015) planes. A weak peak is seen at 24.7° which is also characteristic of the α' form.⁵⁷

The sample recrystallized at 120 °C presents a shift of the two most intense peaks to 16.7° and 19.1°. Moreover these samples show an increase in the intensity of the peaks at 12.3° and 22.2° and the appearance of peaks at 20.8°, 23.0°, 24.0° and 25.1° which are fully characteristic of the α form. These data confirm the formation of the α' form at low crystallization temperature (below 100 °C) and of the α form at higher crystallization temperature (above 120 °C).^{54–56}

The formulated crystallized PLA presented similar WAXD patterns to the neat PLA and the peaks at 9.7° and 28.6° (not shown) characteristic of the talc. Whatever the crystallization temperature and time, the formulated samples showed similar 2θ values and intensities. As shown in Fig. 5, the profile seems similar to that of neat PLA recrystallized at 90 °C but a slight shift of the peak from 18.9° to 19.0° and the appearance of a peak at 23.8° are noticed. To conclude, the WAXD pattern seems to be a combination of α and α' forms whatever the crystallization temperature and time used for the formulated samples.

Therefore, contrary to neat PLA which presents a distinct crystal structure according to the crystallization temperature, the formulated PLA seems not to be affected by the annealing conditions at 85 and 100 °C by crystallizing under a combination of α and α' forms. This absence of modification induced by the formulation and the different annealing conditions is confirmed by Xiao *et al.*⁵³ in the case of triphenyl phosphate and by Piorkowska *et al.*⁶³ with poly(ethylene glycol) and poly(propylene glycol).

Non-annealed neat PLA displays a moderate Young's modulus and maximum stress and a low elongation at break (Fig. 6).^{47,64–66} As shown in Table 1, the recrystallization of neat PLA induces no significant modification of the mechanical properties. The recrystallized neat PLA shows brittle fracture. The elongations at break are below 5% and the maximum stresses are around 50 MPa whatever the recrystallization temperature. As expected, the formulation with 17 wt% of ATBC and 1 wt% of talc leads to a dramatic rise in the elongation at break and a decrease in the maximum stress which reach 477% and 15.8 MPa respectively (Fig. 6).^{44,47,48,67} The result is due to the addition of plasticizer which facilitates polymer chain slippage during the tensile tests.⁴³

Contrary to neat PLA, formulated PLA shows modification in the mechanical properties upon increase of the crystallinity degree.

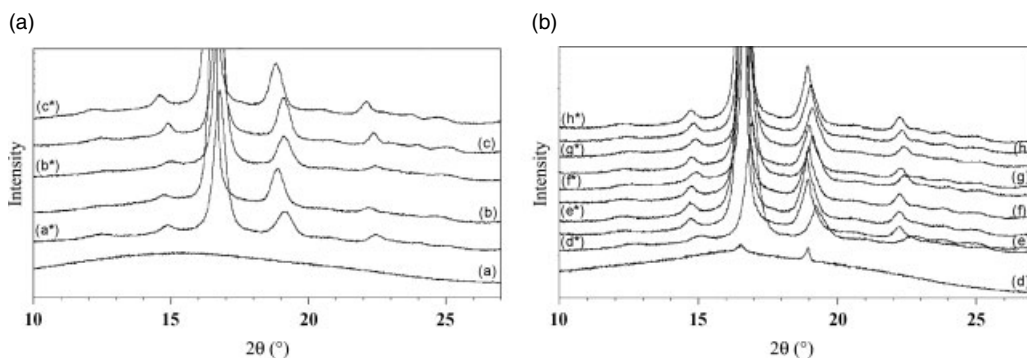


Figure 5. WAXD patterns for (a) neat PLA and (b) formulated PLA before and after contact with EA. The labelling corresponds to the notation in Table 1. The samples after contact are noted with an asterisk.

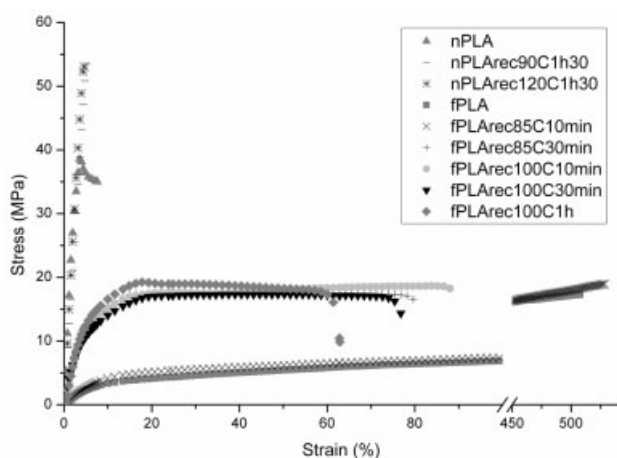


Figure 6. Stress-elongation curves of neat (nPLA) and formulated PLA (fPLA).

At around 30% crystallinity, the annealed formulated samples show an elongation at break divided by 8 compared with the non-annealed formulated PLA. Moreover the maximum stresses remain steady whereas Young's moduli increase with the recrystallization conditions.

According to Kulinski and Piorkowska,⁴³ the diverse lamellae orientations induce different local stresses and strains which may lead to localized fractures. These fractures weaken the plasticized material, which provokes a decrease in the elongation at break. Moreover it has been observed that crystallization of the plasticized PLA exudes the plasticizer into the amorphous phase at the interspherulitic boundaries and at the spherulite peripheries.⁶³ This significant local concentration of plasticizer may weaken the links between lamellae or among neighbouring spherulites, thus causing fissures in the case of stress.

Effect of crystallization on the barrier properties

The helium and oxygen transport coefficients and the EA diffusion and apparent solubility coefficients are listed in Table 3. The well-known Eqn (4) makes it possible to link the permeability coefficient P of helium or oxygen to a kinetic parameter, the diffusion coefficient D , and to a thermodynamic parameter, the solubility coefficient S . D is related to the polymer structure and takes into account the free volume of the matrix and the tortuosity. S is dependent on the solubility of the gas molecules or aroma compounds in the material. Helium is considered as an inert gas,

contrary to oxygen which may interact with the polymer and additives. EA is an organic vapour, and miscible with PLA and ATBC.

As shown in Table 3, the helium permeability coefficients of the non-annealed neat PLA are not significantly modified by the addition of plasticizer and nucleating agent. This is probably due to the low interaction of helium with the matrix and the plasticizer. The crystallization of neat PLA samples induces a significant decrease of the helium permeability coefficient although it keeps the same order of magnitude. This trend is not retrieved in the case of crystallized formulated PLA. The decrease in the gas permeability coefficients is often explained in the literature⁶⁸ by the inclusion of spherulites in the polymer matrix. These impermeable spherulites diminish the amorphous fraction through which the gas molecules can permeate and then affect the gas solubility. Moreover the crystals increase the tortuosity of the gas molecule routes and consequently modify their diffusion coefficients.

Contrary to expectations, the apparent helium diffusion coefficient has an approximate value of $3 \times 10^{-11} \text{ m}^2 \text{ s}^{-1}$ in neat PLA and seems to increase with crystallization up to $1 \times 10^{-10} \text{ m}^2 \text{ s}^{-1}$. However, in accordance with expectation, the increase in crystallinity degree of the samples probably affected the apparent solubility coefficient which slightly decreased from 7×10^{-6} to $0.7 \times 10^{-6} \text{ Pa}^{-1}$ upon crystallization.

The value of the oxygen permeability of neat non-annealed PLA (Table 3) is in agreement with the literature.^{7,9,13,69} The corresponding diffusion coefficient is close to those obtained by Sawada *et al.*^{8,70} at 35°C but less than those given by Bao *et al.*⁶⁹ for an amorphous sample at 30°C . In contrast to helium, the oxygen transport coefficients vary with the formulation. The oxygen permeability and diffusion coefficient doubled and even quadrupled respectively for formulated PLA compared with neat PLA. The oxygen transport properties are affected by the test temperature, which is close to the T_g for the formulated PLA. This may induce an increase of the transport coefficients. Moreover, according to the literature, the diffusion of the gas molecules is closely linked to the free volume of the amorphous phase. Consequently, the rise in the free volume linked to the formulation might induce an increase in the diffusion coefficient and consequently in the permeability coefficient of oxygen for the non-annealed PLA.^{47,71–73}

As expected and noticed for helium, the crystallization of neat PLA samples induces a decrease in the oxygen permeability coefficient although it keeps the same order of magnitude. This evolution is not directly linked to crystalline form since,

Table 3. Helium (He) and oxygen (O₂) permeability and oxygen and EA diffusion and solubility coefficients in neat and formulated PLA before and after recrystallization

Samples	Recrystallization conditions	Eq. χ (%)	Crystalline form	$P_{He} \times 10^{18}$ (m ³ m m ⁻² s ⁻¹ Pa ⁻¹)	$P_{O_2} \times 10^{18}$ (m ³ m m ⁻² s ⁻¹ Pa ⁻¹)	$D_{O_2} \times 10^{12}$ (m ² s ⁻¹)	$S_{O_2} \times 10^6$ (m ³ m ⁻³ Pa ⁻¹)	$D_{EA} \times 10^{17}$ (m ² s ⁻¹)	$S_{EA} \times 10^6$ (m ³ m ⁻³ Pa ⁻¹)
Neat PLA	Non-annealed	3 ± 1	–	100.9 ± 6.4 ^a	2.30 ± 0.09 ^a	1.37 ± 0.29 ^a	1.7 ± 0.3 ^a	2.4	1.3 × 10 ⁻¹
	90 °C, 90 min	36 ± 2	α'	88.2 ± 6.9 ^b	1.96 ± 0.08 ^b	2.21 ± 0.01 ^a	0.9 ± 0.1 ^b	n.d.	1.2 × 10 ⁻¹
	120 °C, 90 min	43 ± 1	α	70.7 ± 1.4 ^c	1.32 ± 0.16 ^b	2.05 ± 0.60 ^a	0.7 ± 0.1 ^b	1.6	n.d.
PLA–2 wt% talc	Non-annealed	6 ± 1	–	110.2 ± 8.9	2.17 ± 0.02	2.02 ± 0.68	1.1 ± 0.1	n.d.	n.d.
PLA–17 wt% ATBC	Non-annealed	2 ± 1	–	98.0 ± 6.7	5.01 ± 0.29	3.71 ± 0.67	1.4 ± 0.2	n.d.	n.d.
Formulated PLA (PLA–1 wt% talc–17 wt% ATBC)	Non-annealed	2 ± 1	–	106.6 ± 11.2 ^a	4.49 ± 0.95 ^a	6.03 ± 1.38 ^a	0.8 ± 0.2 ^a	1 × 10 ⁴	14.5
	85 °C, 30 min	39 ± 1	α, α'	97.6 ± 14.7 ^a	7.10 ± 0.12 ^b	7.49 ± 0.12 ^a	1.0 ± 0.1 ^a	5 × 10 ⁴	15.2
	100 °C, 30 min	38 ± 2	α, α'	99.0 ± 6.5 ^a	6.84 ± 0.92 ^b	8.10 ± 0.98 ^a	0.8 ± 0.1 ^a	n.d.	n.d.
	100 °C, 1 h	37 ± 1	α, α'	100.9 ± 7.8 ^a	7.62 ^b	9.65 ^a	0.8 ^a	7 × 10 ⁴	9.4

The helium and oxygen data of PLA with 2 wt% of talc and PLA with 17 wt% of ATBC are given as references. n.d., not determined.

^{a,b,c} Significant differences at $P < 0.05$ (Fischer). Statistical analysis was carried out separately for neat PLA and formulated PLA.

despite different crystalline structures, both neat recrystallized PLAs present similar diffusion coefficients.

In contrast to neat PLA, the oxygen permeability coefficient of formulated PLA increases slightly with crystallization. Crystallization in formulated PLA may induce plasticizer segregation towards the amorphous phase leading to an increase of approximately 30% of the plasticizer content in the remaining amorphous phase. Courgneau *et al.*⁵¹ showed that the oxygen permeability in amorphous PLA evolves with the plasticizer content. Consequently the enhanced oxygen permeability confirms the plasticizer enrichment of the amorphous phase with the crystallization of formulated PLA. Moreover, according to Kulinski and Piorkowska,⁴³ the presence of a high content of plasticizer could induce accumulation of plasticizer outside the growing spherulites causing weakness of interspherulitic boundaries. Different local stresses and strains may lead to localized crazing cracks creating routes for transport of the gaseous molecules. This increase in the oxygen permeability may confirm the weakness of the crystallized formulated PLA observed previously by tensile tests. No significant modification of the oxygen diffusion coefficient was noticed with crystallization for neat or formulated PLAs, though. This surprising result might be caused by a dedensification of the amorphous phase or by the appearance of a rigid amorphous fraction created by the PLA crystallization. This dedensification phenomenon has been shown by several authors for PET^{74–76} and Poly(ethylene naphthalene) PEN⁷⁷ and suggested for PLA.¹¹ For instance, Hu *et al.*⁷⁷ showed that the decrease in amorphous phase density of PEN, resulting from crystallization, caused a significant rise in oxygen diffusion and solubility coefficients of the amorphous phase, thus hindering the improvement of the gas barrier properties of the material. The concept of three phases with a mobile amorphous fraction (MAF), a rigid amorphous fraction (RAF) and a crystalline fraction has also been suggested to explain the evolution of the oxygen diffusion coefficient. In the heterogeneous stack model, the RAF is located between adjacent lamellae within spherulites and hence the MAF is at the interspherulitic boundaries.⁷⁸ Drieskens *et al.*⁶⁸ suggested that the RAF was less dense than the MAF which could create preferential ways for oxygen molecules through the PLA samples. According to Sawada *et al.*,⁷⁰ increase in the crystallinity degree, i.e. the arrangement of the polymer chains in lamellae, induces the formation of a con-

tinuous pathway. In the case of a gas molecule whose volume is smaller than the interlamellar space, diffusion would be facilitated. They showed an increase in permeation for H₂, O₂, N₂ and CH₄ in PLA up to 20% of crystallinity, and a slow decrease starting around 40%. They explained this behaviour by the junction of crystal lamellae.⁷⁰ In our case a decrease of the diffusion coefficient with higher degree of crystallinity was not observed in the case of the neat samples.

We showed furthermore that the oxygen solubility coefficients of neat PLA decrease with increase in the crystallinity degree but *without* being affected by the crystalline type (α versus α' form). The decrease of the solubility coefficient is an expected result, considering that the creation of crystalline structure lowers the amount of amorphous phase available for gas sorption. Such behaviour has also been experimentally observed in the case of PET.^{78,79}

These effects of the crystallization on the diffusion and solubility coefficient contradict the previous results of Drieskens *et al.*,⁶⁸ who reported an oxygen diffusion coefficient divided by 5 and an oxygen solubility coefficient multiplied by 3 with increase of crystallinity degree from 0 to around 40%. However, the results of gas solubility are in accordance with Sawada *et al.*⁷⁰ who showed a slight decrease of oxygen solubility with crystallization.

Experiments were then carried out with a far more interacting molecule, EA. Already sorption experiments showed a large influence of formulation on the sorption coefficient, which increased by 2 orders of magnitude compared with neat samples probably due to miscibility of EA with ATBC. However, the crystallization of neat and formulated PLA did *not* modify the apparent EA solubility coefficient. The constancy of the apparent solubility coefficient despite the annealing of neat and formulated PLA is not consistent with the Henry sorption model.¹¹ This suggests that at 0.2 activity of EA the structure of the samples is modified during the experiment by contact with the organic compound. As reported by Colomines *et al.*¹¹ and Naga *et al.*,⁷⁹ the contact with organic vapours such as EA leads to plasticization and crystallization (solvent induced crystallization) of the samples.

As in the case of oxygen, the EA diffusion coefficient in neat PLA was not modified by crystallization. The annealing of the formulated samples showed even a slight increase in the EA diffusion coefficient, although values stayed of the same order of

magnitude. In the EA case, the dedensification hypothesis seemed to be unlikely due to the size of the molecule. Therefore the effect of EA on the PLA structure was investigated more thoroughly by conditioning the different samples in an EA atmosphere at 0.2 activity.

Data on the glass transition and crystallinity degree are given in Table 2. The glass transition was measured during the first heating scan although the enthalpic relaxation peak was superposed on the T_g signal. As already observed by Colomines *et al.*¹¹ EA acts as a plasticizer of PLA, which causes T_g shift near to or even below the measuring temperature of the sorption experiment, i.e. 23 °C. The sorption measurement is in this case done in the glass transition region which most probably explains the observed increase of the diffusion coefficient. Moreover, as shown by Colomines *et al.*,¹¹ the thermal recrystallization did not induce any difference in the decrease in T_g of the neat PLA, whereas a gap of 5 °C is seen between the non-annealed and the annealed formulated PLA.

The assessment of the crystallinity degree shows for the non-annealed samples a strong increase in crystallinity. In order to further study the EA induced crystallization, samples were conditioned in an EA atmosphere at higher activity (0.5) and crystallinity was analysed by DSC and WAXD. The results are summarized in Table 2 and Fig. 5. The non-annealed neat sample showed a single melting peak in DSC which may be attributed to the formation of the α form by EA contact. This behaviour was confirmed by WAXD which showed the appearance of peaks characteristic of the α form.

In contrast, no modification of the crystallinity degree was observed for the annealed neat PLA, either by DSC or by WAXD. Moreover, these samples exhibit, after EA contact, thermograms and WAXD patterns similar to those before contact, which means that no modification of the crystal structure is induced by EA contact for the annealed neat PLA.

The non-annealed formulated PLA crystallized up to 21% whereas the annealed formulated PLA did not show any increase in crystallinity degree. The WAXD pattern of non-annealed formulated PLA showed intense peaks after EA vapour contact in agreement with the induced crystallization having both α and α' form crystals. No significant modification was observed on the annealed and formulated PLA pattern which means that the EA contact did not modify the structure of the formulated PLA previously crystallized.

CONCLUSIONS

Crystallization of neat and formulated P(D,L)LA was investigated regarding its impact on barrier properties. Different types of behaviour are noticed according to the probe molecule. In particular, helium is sensitive to the density variation between amorphous and crystalline phases of the polymer matrix, oxygen to the free volume of the amorphous phase and EA presents a high chemical interaction with the polymer.

Hence the helium permeability coefficient decreased with crystallization and was found to be independent of the polymer formulation. Two different behaviours were observed for oxygen transport coefficients. (i) In the case of neat PLA, the permeability coefficient slightly decreases whereas the diffusion coefficient increases with the crystallinity. This behaviour may be explained by the dedensification of the interspherulitic amorphous phase which creates pathways for the oxygen molecules. (ii) In the case of formulated PLA, the permeability coefficient increases upon crystallization due to the plasticizer enrichment of the amorphous

phase, resulting in an increase in the oxygen diffusion coefficient. No impact of PLA polymorphism (α and α' form) on gas barrier properties was observed in this work for the two probe molecules. The behaviour of PLA with EA is much more complex because of its interaction with the matrix. The vapour contact with this organic molecule induces the plasticization and the crystallization of amorphous neat PLA in the α form and in a combination of the α and α' form in the case of non-annealed formulated PLA. Consequently, in comparison with annealing, the contact with EA vapour appears an easy and innovative way to crystallize PLA into the α form.

The relationship barrier properties–PLA microstructure is complex and dependent on the probe used. To reach a consensus between authors and a clear conclusion, work still needs to be pursued in order to understand the effect of the PLA microstructure on gas barrier properties. Moreover our work highlights the importance of considering the chemical interaction of organic vapours with the PLA structure in the development of PLA commodity applications.

ACKNOWLEDGEMENTS

The authors thank Cédric Plessis (INRA, UMR 1145) and Jonathan Idrac (LNE, Trappes) for their technical insight and support. The authors are also grateful to Olivier Vitrac (INRA, UMR 1145) for his support in computer programming.

REFERENCES

- Bogaert J-C and Coszach P, *Macromol Symp* **153**:287–303 (2000).
- Ikada Y and Tsuji H, *Macromol Rapid Comm* **21**:117–132 (2000).
- Gupta AP and Kumar V, *Eur Polym J* **43**:4053–4074 (2007).
- Shen L, Haufe J and Patel MK, *PROBIP 2009, Product Overview and Market Projection of Emerging Bio-Based Plastics*. Report commissioned by EPNOE and European Bioplastics <http://www.epnoe.eu> (2009).
- Dury-Brun C, Chalier P, Desobry S and Voilley A, *Food Rev Int* **23**:199–255 (2007).
- Berlinet C, Brat P and Ducruet V, *Packag Technol Sci* **21**:279–286 (2008).
- Auras R, Harte B and Selke S, *J Appl Polym Sci* **92**:1790–1803 (2004).
- Komatsuka T, Kusakabe A and Nagai K, *Desalination* **234**:212–220 (2008).
- Petersen K, Nielsen PV and Olsen MB, *Starch/Stärke* **53**:356–361 (2001).
- Auras R, Singh SP and Singh JJ, *Packag Technol Sci* **18**:207–216 (2005).
- Colomines G, Ducruet V, Courgneau C, Guinault A and Domenek S, *Polym Int* **59**:818–826 (2010).
- Cava D, Giménez E, Gavara R and Lagaron JM, *J Plast Film Sheet* **22**:265–274 (2006).
- Sanchez-Garcia MD, Gimenez E and Lagaron JM, *J Plast Film Sheet* **23**:133–148 (2007).
- Auras R, Harte B and Selke S, *J Sci Food Agr* **86**:648–656 (2006).
- Mauricio-Iglesias M, Peyron S, Chalier P and Gontard N, *J Food Eng* **109**:9–15 (2011).
- Haugaard V, Weber C, Danielsen B and Bertelsen G, *Eur Food Res Technol* **214**:423–428 (2002).
- Michaels AS and Bixler HJ, *J Polym Sci* **50**:393–412 (1961).
- Kanehashi S, Kusakabe A, Sato S and Nagai K, *J Membrane Sci* **365**:40–51 (2010).
- Sarasua J-R, Prud'homme RE, Wisniewski M, Borgne AL and Spassky N, *Macromolecules* **31**:3895–3905 (1998).
- Miyata T and Masuko T, *Polymer* **39**:5515–5521 (1998).
- Di Lorenzo ML, *Macromol Symp* **234**:176–183 (2006).
- Pluta M and Galeski A, *J Appl Polym Sci* **86**:1386–1395 (2002).
- Ling X and Spruiell JE, *J Polym Sci Pol Phys* **44**:3378–3391 (2006).
- Ling XY and Spruiell JE, *J Polym Sci Pol Phys* **44**:3200–3214 (2006).
- Xiao H, Lu W and Yeh J-T, *J Appl Polym Sci* **113**:112–121 (2009).
- Lai W-C, Liao W-B and Lin T-T, *Polymer* **45**:3073–3080 (2004).
- Li Y, Wu H, Wang Y, Liu L, Han L, Wu J, *et al*, *J Polym Sci Pol Phys* **48**:520–528 (2010).
- Anderson KS and Hillmyer MA, *Polymer* **47**:2030–2035 (2006).

- 29 Schmidt SC and Hillmyer MA, *J Polym Sci Pol Phys* **39**:300–313 (2001).
- 30 Nam JY, Okamoto M, Okamoto H, Nakano M, Usuki A and Matsuda M, *Polymer* **47**:1340–1347 (2006).
- 31 Harris AM and Lee EC, *J Appl Polym Sci* **107**:2246–2255 (2008).
- 32 Kawamoto N, Sakai A, Horikoshi T, Urushihara T and Tobita E, *J Appl Polym Sci* **103**:198–203 (2007).
- 33 Liao R, Yang B, Yu W and Zhou C, *J Appl Polym Sci* **104**:310–317 (2007).
- 34 Li H and Huneault MA, *Polymer* **48**:6855–6866 (2007).
- 35 Ke T and Sun X, *J Appl Polym Sci* **89**:1203–1210 (2003).
- 36 Martin O and Averous L, *Polymer* **42**:6209–6219 (2001).
- 37 Ljungberg N and Wesslén B, *J Appl Polym Sci* **86**:1227–1234 (2002).
- 38 Ljungberg N and Wesslén B, *Biomacromolecules* **6**:1789–1796 (2005).
- 39 Pillin I, Montrelay N and Grohens Y, *Polymer* **47**:4676–4682 (2006).
- 40 Martino VP, Ruseckaite RA and Jiménez A, *J Therm Anal Calorim* **86**:707–712 (2006).
- 41 Martino VP, Jiménez A and Ruseckaite RA, *J Appl Polym Sci* **112**:2010–2018 (2009).
- 42 Kulinski Z, Piorkowska E, Gadzinowska K and Stasiak M, *Biomacromolecules* **7**:2128–2135 (2006).
- 43 Kulinski Z and Piorkowska E, *Polymer* **46**:10290–10300 (2005).
- 44 Baiardo M, Frisoni G, Scandola M, Rimelen M, Lips D, Ruffieux K, *et al*, *J Appl Polym Sci* **90**:1731–1738 (2003).
- 45 Jacobsen S and Fritz HG, *Polym Eng Sci* **39**:1303–1310 (1999).
- 46 Hu Y, Hu YS, Topolkaraev V, Hiltner A and Baer E, *Polymer* **44**:5681–5689 (2003).
- 47 Coltelli M-B, Maggiore ID, Bertoldo M, Signori F, Bronco S and Ciardelli D, *J Appl Polym Sci* **110**:1250–1262 (2008).
- 48 Labrecque LV, Kumar RA, Davé V, Gross RA and McCarthy SP, *J Appl Polym Sci* **66**:1507–1513 (1997).
- 49 EFSA, *EFSA J* **273**:1–26 (2006).
- 50 2002/72/EC Commission Directive of 6 August 2002 relating to plastic materials and articles intended to come into contact with foodstuffs, *TE Commission, Official Journal* **220**: 18–58 (2002).
- 51 Courgneau C, Domenek S, Guinault A, Averous L and Ducruet V, *J Polym Environ* **19**:362–371 (2011).
- 52 Fischer EW, Sterzel HJ and Wegner G, *Kolloid ZZ Polymere* **251**:980–990 (1973).
- 53 Xiao HW, Li P, Ren X, Jiang T and Yeh J-T, *J Appl Polym Sci* **118**:3558–3569 (2010).
- 54 Pan P and Inoue Y, *Prog Polym Sci* **34**:605–640 (2009).
- 55 Kawai T, Rahman N, Matsuba G, Nishida K, Kanaya T, Nakano M, *et al*, *Macromolecules* **40**:9463–9469 (2007).
- 56 Zhang J, Tashiro K, Tsuji H and Domb AJ, *Macromolecules* **41**:1352–1357 (2008).
- 57 Pan P, Kai W, Zhu B, Dong T and Inoue Y, *Macromolecules* **40**:6898–6905 (2007).
- 58 Xiao h, Liu F, Jiang T and Yeh J-T, *J Appl Polym Sci* **117**:2980–2992 (2010).
- 59 Lim LT, Auras R and Rubino M, *Prog Polym Sci* **33**:820–852 (2008).
- 60 Harris AM and Lee EC, *J Appl Polym Sci* **115**:1380–1389 (2010).
- 61 Shieh Y-T and Liu G-L, *J Polym Sci Pol Phys* **45**:466–474 (2007).
- 62 Cho J, Baratian S, Kim J, Yeh F, Hsiao BS and Runt J, *Polymer* **44**:711–717 (2003).
- 63 Piorkowska E, Kulinski Z, Galeski A and Masirek R, *Polymer* **47**:7178–7188 (2006).
- 64 Auras R, Harte B and Selke S, *Macromol Biosci* **4**:835–864 (2004).
- 65 Jia Z, Tan J, Han C, Yang Y and Dong L, *J Appl Polym Sci* **114**:1105–1117 (2009).
- 66 Murariu M, Ferreira ADS, Alexandre M and Dubois P, *Polym Adv Technol* **19**:636–646 (2008).
- 67 Yu J, Wang N and Ma X, *Biomacromolecules* **9**:1050–1057 (2008).
- 68 Drieskens M, Peeters R, Mullens J, Franco D, Lemstra PJ and Hristova-Bogaerds DG, *J Polym Sci Pol Phys* **47**:2247–2258 (2009).
- 69 Bao L, Dorgan JR, Knauss D, Hait S, Oliveira NS and Marucchio IM, *J Membrane Sci* **285**:166–172 (2006).
- 70 Sawada H, Takahashi Y, Miyata S, Kanehashi S, Sato S and Nagai K, *Trans Mater Res Soc Japan* **35**:241–246 (2010).
- 71 McGonigle E-A, Liggat JJ, Pethrick RA, Jenkins SD, Daly JH and Hayward D, *Polymer* **42**:2413–2426 (2001).
- 72 Ahn J, Chung W-J, Pinnau I and Guiver MD, *J Membrane Sci* **314**:123–133 (2008).
- 73 Jang J and Lee DK, *Polymer* **45**:1599–1607 (2004).
- 74 Hu YS, Hiltner A and Baer E, *J Appl Polym Sci* **98**:1629–1642 (2005).
- 75 Qureshi N, Stepanov EV, Schiraldi D, Hiltner A and Baer E, *J Polym Sci Pol Phys* **38**:1679–1686 (2000).
- 76 Lin J, Shenogin S and Nazarenko S, *Polymer* **43**:4733–4743 (2002).
- 77 Hu YS, Liu RYF, Zhang LQ, Rogunova M, Schiraldi DA, Nazarenko S, *et al*, *Macromolecules* **35**:7326–7337 (2002).
- 78 del Rio J, Etxeberria A, Lopez-Rodriguez N, Lizundia E and Sarasua JR, *Macromolecules* **43**:4698–4707 (2010).
- 79 Naga N, Yoshida Y, Inui M, Noguchi K and Murase S, *J Appl Polym Sci* **119**:2058–2064 (2011).